DOI: 10.1093/brain/awh201 *Brain* (2004), **127,** 1785–1795

Brainstem neurodegeneration correlates with clinical dysfunction in SCA1 but not in SCA2. A quantitative volumetric, diffusion and proton spectroscopy MR study

L. Guerrini,[1] F. Lolli,[2] A. Ginestroni,[2] G. Belli,[3] R. Della Nave,[1] C. Tessa,[1] S. Foresti,[1] M. Cosottini,[4] S. Piacentini,[2] F. Salvi,[5] R. Plasmati,[5] D. De Grandis,[6] G. Siciliano,[4] A. Filla[7]and M. Mascalchi[1]

[1]*Radiodiagnostic Section, Department of Clinical Physiopathology,* [2]*Neurological Clinic, Department of Neurological Sciences, University of Florence,* [3]*Department of Physics, Careggi Hospital, Florence,* [4]*Department of Neurology, University of Pisa,* [5]*Division of Neurology, Bellaria Hospital, Bologna,* [6]*Division of Neurology, General Hospital, Rovigo and* [7]*Division of Neurology, University of Naples, Naples, Italy*

Correspondence to: Mario Mascalchi, Radiodiagnostic Section, Department of Clinical Physiopathology, University of Florence, Viale Morgagni 85, Florence, Italy
E-mail: m.mascalchi@dfc.unifi.it

Summary

Magnetic resonance (MR) techniques enable *in vivo* measurement of the atrophy of the brainstem and cerebellum in spinocerebellar ataxia type 1 (SCA1) and 2 (SCA2) patients, which is accompanied by a decrease in the concentration of *N*-acetyl aspartate (NAA) or of the NAA/creatine ratio in the pons and cerebellum. Mean diffusivity ($\bar{D}$) is emerging as an additional sensitive and quantitative MR parameter to investigate brain diseases. In order to explore differences between the MR features of SCA1 and SCA2 and correlate the MR and clinical findings in the two conditions, we examined 16 SCA1 patients, 12 SCA2 patients and 20 healthy control subjects. The MR protocol included T1-weighted 3D gradient echo sequences, single-voxel proton spectroscopy of the right cerebellar hemisphere (dentate and peridentate region) and of the pons with a PRESS sequence and an external reference quantitation method, and (in nine patients with SCA1 and nine patients with SCA2) diffusion-weighted echo-planar images with reconstruction of the $\bar{D}$ maps. The patients were evaluated with the Inherited Ataxia Clinical Rating Scale (IACRS). Compared with control subjects, the SCA1 and SCA2 patients showed a decrease ($P < 0.01$) in the volume of the brainstem and cerebellum and in the concentration of NAA in the pons and cerebellar hemisphere, whereas $\bar{D}$ of the brainstem and cerebellum was increased. No significant difference was observed between the SCA1 and SCA2 patient groups. No correlation between cerebellar volume and dentate and peridentate NAA concentration was found in SCA1 or SCA2 patients. The volume of the brainstem, $\bar{D}$ of the brainstem and cerebellum and the concentration of NAA in the pons were correlated ($P < 0.05$) with the IACRS score in SCA1 but not in SCA2. This discrepancy is in line with the clinical observation that the clinical deficit has a later onset and faster progression in SCA1 and an earlier onset and slower progression in SCA2, and suggests that neurodegeneration of the brainstem is a comparatively more rapid process in SCA1. In conclusion, our study indicates that SCA1 and SCA2 substantially exhibit the same MR features. The correlation in SCA1 between clinical severity and quantitative volumetric, diffusion MRI and proton MR spectroscopy findings in the brainstem indicates that these measurements might be employed for longitudinal studies and hopefully as surrogate markers in future pharmacological trials of this condition.

Keywords: spinocerebellar ataxia; magnetic resonance imaging; diffusion; magnetic resonance spectroscopy *N*-acetyl-aspartate

Abbreviations: ADCA = autosomal dominant cerebellar ataxia; Cho = choline; Cr = creatine; $\bar{D}$ = mean diffusivity; ^{1}H-MRS = proton magnetic resonance spectroscopy; IACRS = Inherited Ataxia Clinical Rating Scale; MR = magnetic resonance;

NAA = *N*-acetyl aspartate; OPCA = olivopontocerebellar atrophy; PCF = posterior cranial fossa; PRESS = point-resolved proton spectroscopy sequence; SCA1 = spinocerebellar ataxia type 1; SCA2 = spinocerebellar ataxia type 2

Received February 12, 2004. Revised March 26, 2004. Accepted March 28, 2004. Advanced Access publication July 7, 2004

Introduction

The spinocerebellar ataxias are a group of autosomal dominant diseases predominantly due to expansion of a CAG triplet encoding polyglutamines (Subramony and Filla, 2001). Spinocerebellar ataxias type 1 (SCA1) and type 2 (SCA2) are the most common types in Italy (Pareyson *et al*., 1999). In patients with SCA1 or SCA2, MRI enables *in vivo* assessment of the volume loss of the cerebellum and brainstem (Burk *et al*., 1996; Schols *et al*., 1997; Klockgether *et al*., 1998*b*) and proton magnetic resonance spectroscopy (^{1}H-MRS) demonstrates a decrease in *N*-acetyl aspartate (NAA) concentration or in the NAA/creatine (Cr) ratio in the cerebellum and pons (Davie *et al*., 1995; Mascalchi *et al*., 1998; Boesch *et al*., 2001). Diffusion MRI is emerging as a sensitive, quantitative and reproducible tool to evaluate brain damage in white and grey matter diseases (Bozzali *et al*., 2001; Cercignani *et al*., 2001; Schocke, 2002; Cercignani *et al*., 2003) and was recently employed in the evaluation of patients with inherited or sporadic progressive ataxias (Della Nave *et al*., 2004).

Prior studies comparing the MRI features in SCA1 and SCA2 were limited to quantitative assessment of atrophy (Burk *et al*., 1996; Klockgether *et al*., 1998*b*). Moreover, the correlation between the MR and clinical findings in patients with spinocerebellar ataxias has not been thoroughly investigated until now.

We compared quantitative volume and diffusion MRI and ^{1}H-MRS findings in two groups of patients with SCA1 or SCA2 and correlated the MR findings with the patients' scores on the Inherited Ataxia Clinical Rating Scale (IACRS) (Filla *et al*., 1990).

Methods

Patient and control populations

Between January 2002 to September 2003, 28 patients with autosomal dominant cerebellar ataxia were defined as SCA1 ($n = 16$; nine women and seven men, mean age 44 ± 9 years, range 29−59) or SCA2 ($n = 12$; three women and nine men, mean age 52 ± 11.8 years, range 33–68) based on the results of genetic tests (Pareyson *et al*., 1999), and gave their informed consent to participation in the study which was approved by the Ethical Committee of the Careggi Hospital University of Florence. They belonged to 22 (11 SCA1 and 11 SCA2) unrelated Italian families. Ten (four men and six women, mean age 44 ± 8 years; range 29–71 years) healthy volunteers without familiar or personal history of neurological diseases served as controls for volumetric MRI and ($n = 6$) quantitative single-voxel ^{1}H-MRS.

Control data for diffusion MRI were obtained in another 20 healthy subjects (eight women and 12 men, mean age 45 ± 11 years).

On the day of the MR examination, the same neurologist performed an extensive clinical evaluation in each patient, with determination of the duration of symptoms (disease duration) based on interview or review of hospital records. After the neurological examination, the score on the Inherited Ataxias Clinical Rating Scale (IACRS) was calculated. In this scale a progressive score with a maximum of 46 points corresponds to a greater neurological deficit, including signs of cerebellar and corticospinal tract involvement (Filla *et al*., 1990).

MRI examinations

All examinations were performed on a 1.5 T system (Gyroscan ACS-NT; Philips Medical System, Best, The Netherlands) equipped with 23 mT/m gradient capability using a standard quadrature head coil, which enables MRI and ^{1}H-MRS.

The MRI acquisition protocol included scout images, sagittal 3 mm thick T1-weighted [repetition time (TR) 400 ms, echo time (TE) 14 ms, number of excitations (NEX) 2] spin echo images and coronal 1 mm thick 3D T1-weighted (TR 25 ms, TE 4.6 ms, flip angle 30°) turbo gradient echo images covering the entire posterior cranial fossa (PCF). Diffusion-weighted MRI was obtained according to a previously reported protocol (Della Nave *et al*., 2004) in 18 patients (nine SCA1, mean age 45 ± 9 years; nine SCA2, mean age 52 ± 12 years) and in the 20 controls. Briefly, 18 contiguous diffusion-weighted slices were acquired on axial planes parallel to the bicommissural line from the medulla to the vertex with a double-shot echo-planar sequence [TR 1600 ms, TE 80 (102) ms, echo-planar imaging factor 15] with peripheral pulse gating. The slice thickness was 6 mm, the field of view 230 mm and the matrix 100 × 256. Diffusion-sensitizing gradients were applied along the three orthogonal axes using a *b* value of 0 and 1000 s/mm^2. For each slice, the manufacturer's software reconstructed the maps of the mean diffusivity ($\bar{D}$) which is the diffusivity derived from three measurements in orthogonal directions.

For quantitative ^{1}H-MRS we employed an external phantom calibration method. The volume of interest (voxel) was a cube of 1.5–2 × 1.5–2 × 1.5–2 cm (4.5–8 ml) placed in the basis pontis and in the right dentate nucleus and surrounding the deep cerebellar hemisphere (Fig. 1). To avoid inclusion of CSF spaces within the volume of interest, the smallest voxel size was employed in patients with overt atrophy. After automatic shimming and gradient tuning, water suppression was obtained with an adiabatic radio frequency (RF) pulse centred around the water peak with a spectral width of 60 Hz, followed by dephasing crusher gradients. The performance of water signal suppression was optimized by fine tuning the flip angle of the water suppression RF pulse slightly in excess of 90° to achieve a minimal residual water signal. A point-resolved proton spectroscopy sequence (PRESS) technique was used for acquisition of the proton spectrum with TR 2000 ms, and 128 measurements were made. With 512 spectral points, each spectrum acquisition time was 4.24 min. For determination of metabolite T2 relaxation time, the spectra were obtained with four TEs (80, 136, 272 and 400 ms) in all patients and controls.

Soon after each examination, a spherical phantom (volume 2.5 litres) containing a 30 mM solution of sodium acetate loaded with

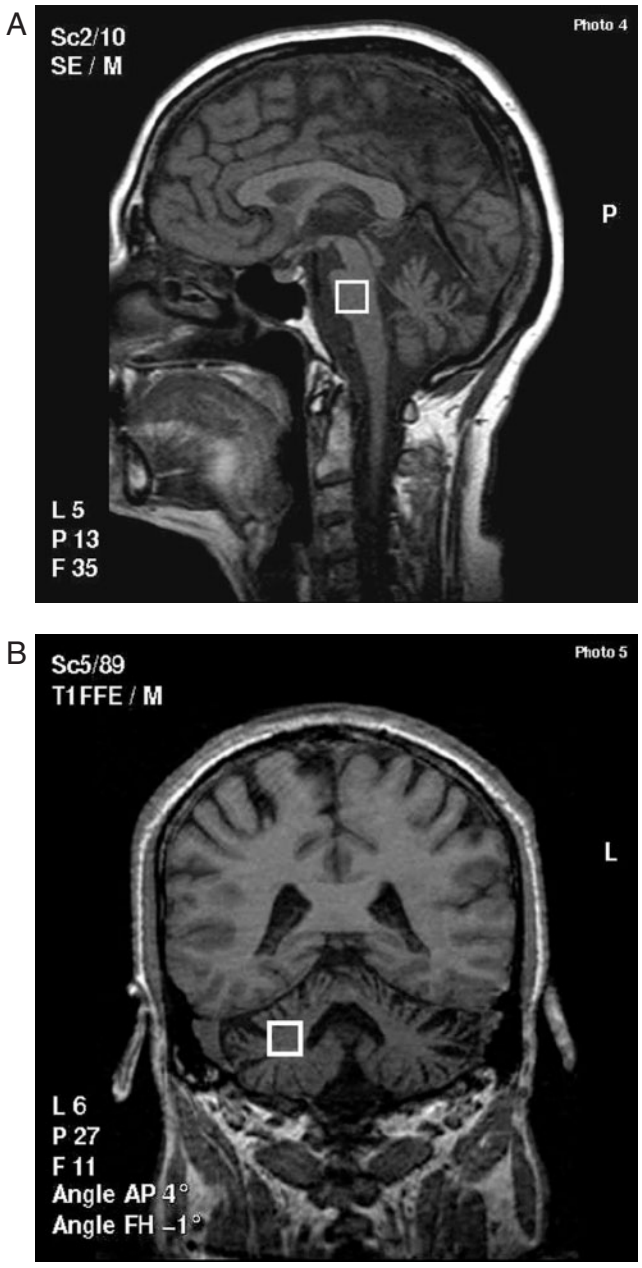

Fig. 1 Sagittal T1-weighted spin echo image (**A**) and coronal T1-weighted gradient echo image (**B**) showing the location of the 4.5 ml volume of interest in the basis pontis and deep right cerebellum in a patient with SCA1. Note the loss of bulk of the brainstem and cerebellum.

4.7 g/litre of sodium chloride was placed within the coil. To prevent regional signal variations due to magnetic field inhomogeneity and eddy currents, a water-suppressed PRESS sequence with TR 2000 and TE 30 ms was obtained with the same geometrical coordinates of each single voxel acquired in the same subject in the cerebellum and pons.

Data analysis

Volumetric MRI

The same operator, who was blind to the genetic, clinical, diffusion MRI and ^{1}H-MRS data, determined the volumes of the cerebellum and of the brainstem and of the posterior cranial fossa on a remote console (Philips Easy Vision, release 4.3). After manual landmark-defined presegmentation, the volumes of cerebellum and brainstem were calculated with a visually supervised automatic procedure in which seeds were dropped on a structure of interest and automatically grown to include all the connected pixels until the whole structure was outlined. The boundaries of the cerebellum and brainstem were defined on coronal oblique 2 mm thick images reformatted in order to be parallel to the floor of ventricle IV. The grey and white matter of the cerebellar vermis and hemispheres were measured from the posterior to the anterior images until the inferior or middle cerebellar peduncles. In the more anterior images, only the cortical grey matter was included in the volume of the cerebellum, whereas the white matter was considered as a portion of the brainstem. Computation of the volume of the vermis was not performed since its separation of the vermis from the cerebellar hemispheres was easy in the anterior portions, due to the sulcus between the vermis and the tonsils, but almost impossible in the posterior portions, where no clear landmark is present. The upper limit of the brainstem was defined by a line perpendicular to the cerebral peduncles traced between the widest portion of the third ventricle, medially, and the lateral surface of the cerebral peduncles, laterally, inclusive of the colliculi (see supplementary material, Fig. 1). The lower limit of the brainstem was defined by a line coinciding with the foramen magnum. For the purpose of normalizing the cerebellar and brainstem volumes to the individual size, the volume of the posterior cranial fossa were evaluated in 5 mm thick reformatted axial images.

To assess intra-operator variability, the measurements of the volumes of the cerebellum and brainstem in one patient were repeated on five different days; the coefficient of variation was 0.7% for the volume of the brainstem and 1.2% for the volume of the cerebellum.

Diffusion MRI

The diffusion-weighted images were processed according to a procedure reported previously (Della Nave *et al*., 2004) by another operator who was blind to the genetic and clinical data and to the volumetric MRI and 1H-MRS findings. Regional $\bar{D}$ was evaluated with round regions of interest in the pons (one, 10 mm in diameter), peridentate white matter (four, 5 mm in diameter, two on the left and two on the right side) and middle cerebellar peduncles (two, 5 mm in diameter, one on each side) avoiding CSF contamination (see supplementary material, Fig. 2). For determination of the $\bar{D}$ values of the entire brainstem and cerebellum and of the cerebral hemispheres, the operator performed a two-step procedure consisting of manual segmentation of the skull to define the intracranial volume followed by application of a threshold to separate brain parenchyma from CSF spaces. In particular, $\bar{D}$ maps of each slice were first manually segmented for the exclusion of scalp soft tissues and skull bone and the definition of intracranial volume. A second manual segmentation was then applied to separate the posterior cranial fossa from the supratentorial intracranial spaces (see supplementary material, Fig. 3). Mean intra-operator coefficient of variation for segmentation of the skull was 2.7% and for determination of the posterior cranial fossa spaces it was 0.5% in 10 measurements taken on different days in the same patient. To exclude CSF spaces from the $\bar{D}$ map histograms, a threshold value of 239 mm^2/s was adopted, which would enable exclusion of 97.5% of the CSF-containing pixels, assuming a Gaussian distribution of the CSF $\bar{D}$ value (Chun *et al*., 2000; Della Nave *et al*., 2004). Histograms of $\bar{D}$ were computed for the

cerebellum and brainstem and for the cerebral hemispheres using a custom-made program (MRIcro 1.27; courtesy of C. Rorden). Since the curve of brain $\bar{D}$ on the histogram was not symmetrical, we measured the median, i.e. the 50th percentile, rather than the mean value of the $\bar{D}$ histograms of the brainstem and cerebellum and of the cerebral hemispheres (Della Nave *et al*., 2004). In addition, for the brainstem and cerebellum histogram, the 25th percentile was calculated, which is expected to be less modified by possible contamination by CSF. Post-processing of the diffusion weighted images required approximately 1 h for each study.

^{1}*H-MRS*

Spectra were preliminarily processed with zero filling, exponential multiplication, Fourier transformation and manual phase correction, and the areas of the peaks at 2.07, 3.00 and 3.20 p.p.m. were assigned to NAA, Cr and choline (Cho). The possible presence of a peak at 1.3 p.p.m. exhibiting the phase reversal at the TE 272 and 136 ms typical of lactate was recorded.

Quantitative analysis was performed according to a previously reported procedure (Mascalchi *et al*., 2002*a*) with AMARES, a non-linear least squares fitting algorithm operating in the time domain (FID signal) (Vanhamme *et al*., 1997), as implemented in the MRUI package (van den Boogaart A *et al*., 1996). A frequency-selective filter centred at 4.7 p.p.m. to reduce the residual of the water signal and exponential multiplication to reduce noise were applied to the FID signal before quantitative processing (Van den Boogaart *et al*., 1994).

The area of the acetate peak, $S_{ac,}$ was used to calculate metabolite concentrations, C_{met}, from the measured metabolite peak area according to the expression

$$C_{met} = C_{ac}(S_{met}/S_{me})N_{ac}/N_{met}$$

where $C_{ac} = 30$ mM, $N_{ac} = 3$ and N_{met} is the number of protons contributing to the metabolite peak.

For each spectrum a correction was performed for different coil loading, transmit and receive gain between the *in vivo* and the phantom measurements and for the T2 effects measured as indicated below. No correction for blood vessels and CSF spaces were made. The concentrations were expressed as millimoles per litre.

The T2 relaxation times of NAA, Cr and Cho in the cerebellum and pons were determined by fitting the two-parameter (amplitude S_0, decay constant 1/T2) mono-exponential

$$S(\tau)S_0e^{-TE/T2}$$

to the data using a linear least squares algorithm.

To assess intra-operator variability, the concentrations and T2 relaxation times in the cerebellar spectrum of one patient were determined on five different days. The coefficient of variation was below 5% for all the measurements.

Statistical analysis

We employed the non-parametric Mann–Whitney *U* test for preliminary assessment of differences between patients (SCA1 and SCA2) and controls and between the two patient groups for age, disease duration and IACRS scores.

The same test was then employed for the differences between the three groups in the volume of the PCF, the cerebellar and brainstem volumes normalized to PCF, the regional and histogram $\bar{D}$ values, and the concentration and T2 relaxation time of NAA, Cr and Cho in the cerebellum and pons.

The Pearson correlation (r) was calculated to assess the correlation between disease duration and IACRS scores on the one hand and the brainstem and cerebellar volumes, $\bar{D}$ and NAA concentrations in the groups of SCA1 and SCA2 patients, separately. In all instances significance was set at $P < 0.05$.

Results

The ages of patients and controls were not significantly different.

The disease duration was significantly ($P < 0.01$) shorter in SCA1 (mean 7.4 ± 4.8 years) than in SCA2 (mean 15.2 ± 12.5 years) patients, whereas the IACRS scores of the SCA1 (mean 11.5 ± 6.5) and SCA2 (mean 14.8 ± 3.0) patients were not significantly different. The disease duration and the IACRS scores were correlated ($P < 0.01$) in SCA1 ($r = 0.69$) but not in SCA2 ($r = 0.32$).

Volumetric MRI

The results of the volumetric evaluation are summarized in Table 1.

The volumes of the cerebellum and brainstem normalized to PCF were significantly ($P < 0.001$) lower in SCA1 and SCA2 patients than in controls. The volume of the cerebellum was smaller in SCA2 than in SCA1 patients but the difference was not statistically significant. The volume of the brainstem in SCA1 and SCA2 patients was similar.

The volumes of the PCF, of the brainstem and the cerebellum in our patients and controls are provided in Table 1 of the supplementary material.

Diffusion MRI

Table 2 details the results of the region of interest and histogram analysis of $\bar{D}$ in SCA1 and SCA2 patients and controls.

Table 1. *Volumetric MRI of the brainstem and cerebellum in patients with SCA1 and SCA2 and healthy subjects*

	SCA1	SCA2	Healthy controls
Volume of brainstem normalized to the PCF	0.11 ± 0.02***	0.11 ± 0.03***	0.15 ± 0.01
Volume of the cerebellum normalized to the PCF	0.49 ± 0.06***	0.41 ± 0.07***	0.60 ± 0.03

PCF = posterior cranial fossa.***$P < 0.001$; all statistically significant P values refer to the difference between SCA1 or SCA2 patients and controls. No statistically significant difference was observed between SCA1 and SCA2 for any of the MRI measurements.

Table 2. $\bar{D}$ *(× 10^{-3} mm^2/s) of the brainstem, cerebellum and cerebral hemispheres in patients with SCA1 and SCA2 and healthy subjects*

	SCA1 ($n = 9$)	SCA2 ($n = 9$)	Healthy controls ($n = 20$)
Region of interest			
Pons	0.80 ± 0.06	0.84 ± 0.12*	0.74 ± 0.11
MCP	1.28 ± 0.11***	1.08 ± 0.22**	0.81 ± 0.14
CWM	1.18 ± 0.05***	1.02 ± 0.21	0.86 ± 0.16
Medulla	0.97 ± 0.09**	0.97 ± 0.11**	0.77 ± 0.16
Histograms			
Brainstem and cerebellum			
25th percentile	0.83 ± 0.08**	0.90 ± 0.07***	0.71 ± 0.6
50th percentile	1.07 ± 0.15**	1.19 ± 0.11***	0.86 ± 0.10
Cerebral hemispheres			
50th percentile	0.91 ± 0.09	0.87 ± 0.04	0.85 ± 0.06

$^{*}P < 0.05$ $^{**}P < 0.01$ $^{***}P < 0.001$; all statistically significant P values refer to the difference between SCA1 or SCA2 patients and controls. No statistically significant difference was observed between SCA1 and SCA2 for any of the MRI measurements. MCP = middle cerebellar peduncles; CWM = cerebellar white matter.

The $\bar{D}$ in the middle cerebellar peduncles and the medulla was increased in the SCA1 and SCA2 patients compared with controls ($P \leqslant 0.01$). The increase in the peridentate white matter $\bar{D}$ was significant ($P = 0.001$) in SCA1 and borderline ($P = 0.05$) in SCA2. The pontine $\bar{D}$ was increased in SCA1 and SCA2 but the differences compared with the controls was statistically significant ($P < 0.05$) for SCA2 only. The 25th and 50th percentiles of the brainstem and cerebellum $\bar{D}$ were ($P < 0.01$) higher in both SCA1 and SCA2 compared with controls (Fig. 2).

The median, i.e. 50th percentile, of the $\bar{D}$ of the supratentorial brain was not statistically different in SCA1, SCA2 and controls.

No significant difference for any $\bar{D}$ measurement was observed between SCA1 and SCA2 patients.

^{1}H-MRS

A lactate peak was observed in the pons of one SCA1 patient only.

Table 3 reports the concentrations and T2 relaxation times of the metabolites in the cerebellum and pons for SCA1 and SCA2 patients and controls. The concentrations of NAA in the cerebellum and pons were significantly ($P < 0.01$) reduced in SCA 1 and SCA2 patients compared with controls. No significant differences were observed in the cerebellum and pons for the concentrations of Cr and Cho and for the T2 of NAA, Cr and Cho. No significant differences were present between SCA1 and SCA2 patients concerning all the MRS variables.

MR: clinical correlations

The volume of the brainstem ($r = -0.74$), the median of brainstem and cerebellar $\bar{D}$ ($r = 0.70$) and the NAA concentration in the pons ($r = -0.63$) were significantly ($P < 0.05$) correlated to the IACRS score in SCA1, but not in SCA2 patients (Fig. 3).

The volume of the cerebellum was inversely correlated with the duration (years) of disease duration in SCA1 ($r = -0.73$; $P = 0.003$) and in SCA2 ($r = -0.70$, $P = 0.01$). The median of brainstem and cerebellar $\bar{D}$ was correlated with disease duration ($r = 0.84$, $P = 0.004$) in SCA1 only. No other significant correlation was observed.

Discussion

Autosomal dominant cerebellar ataxias (ADCAs) are progressive diseases with an incidence of 1–10/100 000 (Gudmundsson, 1969; van de Warrenburg *et al*., 2002). Since there is no effective therapy, they lead to severe disability and death (Harding and Deufel, 1993). Molecular genetics enables subdivision of autosomal dominant cerebellar ataxias in several types and genotype–phenotype correlation studies (Subramony and Filla, 2001).

SCA1 is associated with a CAG repeat expansion in chromosome 6p encoding a protein of unknown function called ataxin 1, whereas in SCA2 the CAG triplet expansion is located at chromosome 12q, encoding a protein of unknown function called ataxin 2 (Subramony and Filla, 2001). Clinical features in SCA1 and SCA2 are similar, although signs of corticospinal involvement, pale discs and dysphagia are more frequent in SCA1 and saccade-slowing and depressed tendon reflexes are more frequent in SCA 2 (Burk *et al*., 1996; Schols *et al*., 1997).

In the few cases of SCA1 and SCA2 which came to neuropathological examination, a macroscopic pattern of olivopontocerebellar atrophy (OPCA) with neuronal loss and gliosis in the inferior olives, pons and cerebellum was observed (Durr *et al*., 1995; Gilman *et al*., 1996; Estrada *et al*., 1999). However microscopic examination shows some differences between the two conditions (Iwabuchi *et al*., 1999). In fact, the spinocerebellar and vestibulocerebellar systems and the dentate nucleus

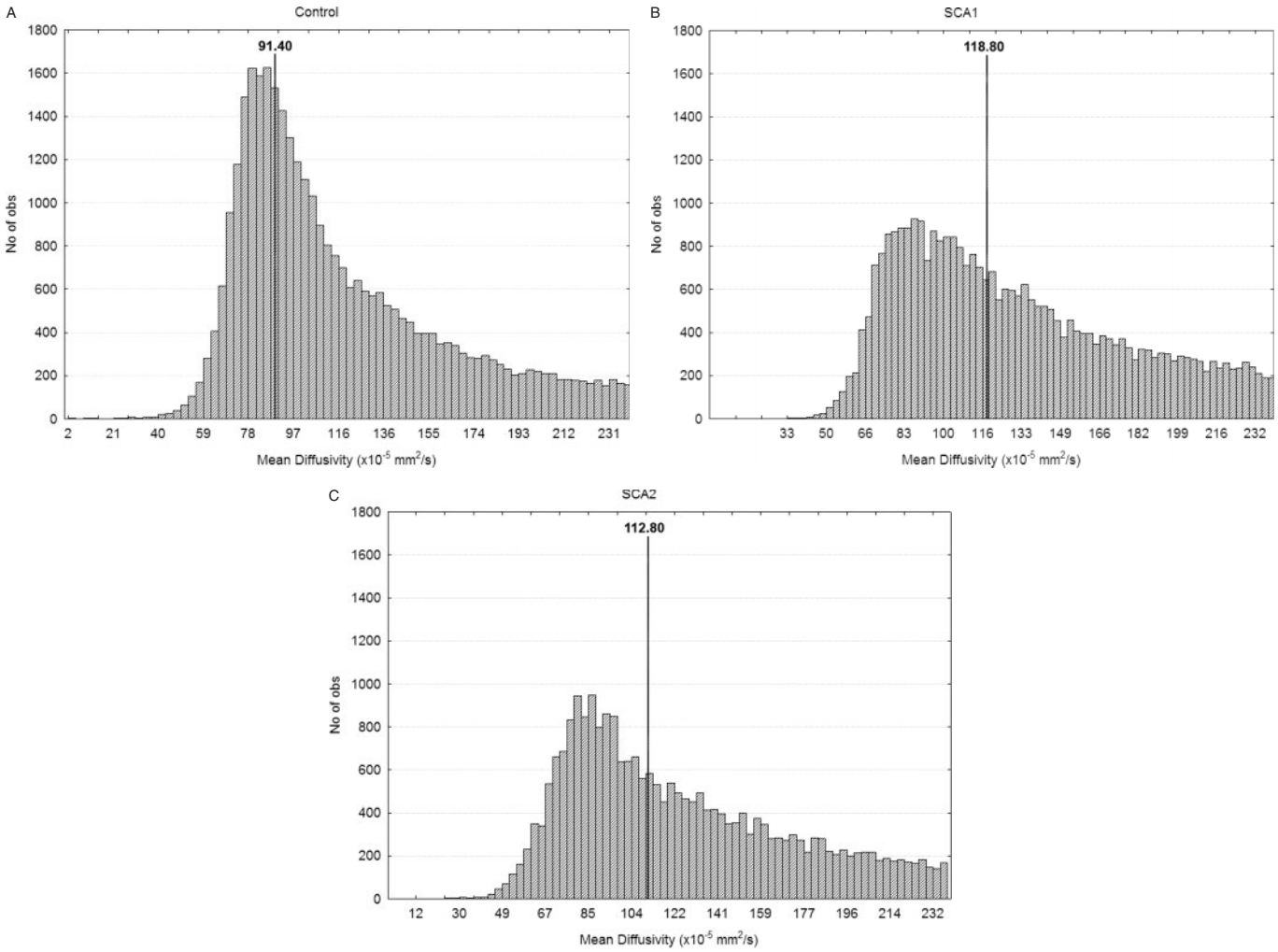

Fig. 2 Histograms of brainstem and cerebellar $\bar{D}$ in one healthy control (**A**), one SCA1 patient (**B**) and one SCA2 (**C**) patient. Note the different shape of the histogram and the rightward displacement of median (vertical line) values in **B** and **C**.

are affected in SCA1 and spared in SCA2, and the cerebellar cortex is more severely damaged in SCA2 than in SCA1.

The features of OPCA on conventional MRI were defined using either subjective evaluation of morphology and the signal intensity of the brainstem and cerebellum (Savoiardo *et al*., 1990; Ormerod *et al*., 1994) or morphometric measurements (Wullner *et al*., 1993; Schols *et al*., 1997; Mascalchi *et al*., 1998; Nagaoka *et al*., 1999). In particular, in hereditary and sporadic OPCA Savoiardo and colleagues reported characteristic thinning of the ventral pons and diffusely increased signal intensity of the brainstem and cerebellar white matter in proton density and T2-weighted images, with sparing of the corticospinal tracts and the superior cerebellar peduncles (Savoiardo *et al*., 1990). These last findings were reported in advanced cases of SCA1 and SCA2 (Mascalchi *et al*., 1998; Giuffrida *et al*., 1999).

The absolute volumes of the cerebellum and brainstem in our normal subjects were in substantial agreement with previous studies (Klockgether *et al*., 1998*b*; Raz *et al*., 2001) The reductions in normalized volumes of the cerebellum and brainstem we observed in SCA1 and SCA2 are in line with the results of a previous study (Klockgether *et al*., 1998*b*) which reported significantly more pronounced atrophy of the cerebellum and brainstem in SCA2 than in SCA1.

The distribution pattern of increased $\bar{D}$ in the brainstem and cerebellum that we observed in our SCA1 and SCA2 patients matched the distribution of the neuropathological changes in OPCA. In particular, $\bar{D}$ was increased throughout the brainstem and cerebellum and was more prominent in the middle cerebellar peduncles, which are the site of the most severe damage in OPCA (Lowe *et al*., 1997). The mild increase in $\bar{D}$ in the pons might be related to inclusion in the region of interest of the corticospinal tracts, which are characteristically spared in OPCA. Although the exact pathological correlate of increase in $\bar{D}$ in SCA1 and SCA2 cannot be established, it probably reflects the wallerian degeneration of the white matter observed in OPCA (Lowe *et al*., 1997).

Diffusion tensor MRI enables evaluation of the fractional anisotropy of the white matter, but was not employed in our

Table 3. *Concentrations (mmol/l) and T2 relaxation times (ms) in the cerebellum and pons in patients with SCA1 or SCA2 and healthy controls*

	SCA1	SCA2	Healthy subjects	*P*
Cerebellum				
Concentration	8.3 ± 2.5	8.3 ± 4.2	14.2 ± 1.6	<0.01
NAA				
T2 relaxation time	357 ± 111	400 ± 103	368 ± 107	NS
Concentration	12.0 ± 2.4	9.3 ± 2.7	13.4 ± 1.8	NS
Cr				
T2 relaxation time	184 ± 4.3	233 ± 54	198 ± 34	NS
Concentration	2.6 ± 0.8	3.3 ± 1.2	2.8 ± 0.5	NS
Cho				
T2 relaxation time	288 ± 70	319 ± 142	331 ± 26	NS
Pons				
Concentration	8.6 ± 2.1	9.4 ± 2.7	14.0 ± 4.7	0.01
NAA				
T2 relaxation time	323 ± 81	365 ± 64	351 ± 46	NS
Concentration	6.2 ± 1.8	5.8 ± 1.4	7.7 ± 3.4	NS
Cr				
T2 relaxation time	165 ± 39	284 ± 138	189 ± 33	NS
Concentration	2.4 ± 0.8	3.2 ± 0.9	3.4 ± 0.8	NS
Cho				
T2 relaxation time	352 ± 68	251 ± 46	305 ± 49	NS

NS = not significant.

study. However, an increase in mean diffusivity was highly correlated with the decrease in diffusion anisotropy in a diffusion tensor MRI study of the internal capsules in patients with primary lateral sclerosis (Ulug *et al*., 2004). This is a neurodegenerative condition in which selective wallerian degeneration of the corticospinal tracts is assumed to be due to dysfunction and loss of the cortical motor neurons (Lowe *et al*., 1997).

In degenerative diseases of the CNS, ^{1}H-MRS shows a decrease in the concentration of the putative neuronal and axonal marker NAA or of the NAA/Cr ratio in the areas where there is maximal neuronal damage and loss on neuropathological examination (Gill *et al*., 1989). Preliminary MRS studies in patients with SCAs included a small number of patients (Davie *et al*., 1995; Mascalchi *et al*., 1998; Boesch *et al*., 2001) and two of them were performed with a semiquantitative approach only (Mascalchi *et al*., 1998; Boesch *et al*., 2001). The decrease in the concentration of NAA we observed in the cerebellum of patients with SCA1 and SCA2 confirms the results of the above studies. Also, the pontine reduction in NAA supports and extends the data obtained with a semiquantitative approach in SCA1 (Mascalchi *et al*., 1998). We observed lower concentrations of Cho and Cr in the pons and of Cr in the cerebellum of SCA1 and SCA2 patients compared with controls, but the differences were not statistically significant. A reduction in Cho has been reported in the cerebellum of ADCA patients (Davie *et al*., 1995) and in the Cho/Cr ratio in the pons of SCA1 patients (Mascalchi *et al*., 1998). At variance with Boesch *et al*. (2001), who observed a lactate peak in all of the four SCA2 patients they examined, we observed a lactate peak in the pons of only one SCA1 patient. Although the single-voxel technique is the standard procedure for clinical quantitative ^{1}H-MRS, it has limited spatial resolution. In fact, with the voxel size employed in this study, it is not possible to separate the dentate nucleus from the surrounding white matter, which contains either fibres connecting the cerebellar cortex to the nucleus and the latter to the brainstem or afferent fibres from the brainstem to the cerebellar cortex. Hence, it is impossible from our data to attribute a decrease in cerebellar NAA to dysfunction of the dentate neurons or to wallerian degeneration of the adjacent fibres due to damage in the cerebellar cortical or brainstem neurons. Also, it is impossible to attribute a decrease in NAA in the pons to damage of a particular grey structure or white matter tract in the brainstem. This notwithstanding, taking into consideration the distribution of the neuropathological changes and the better quality of the pontine spectra compared with those in the medulla (Mascalchi *et al*., 2002*a*), the basis pontis can be chosen as the site of choice for the ^{1}H-MRS evaluation of neurodegeneration of the brainstem in OPCA.

Relaxation times of metabolites can affect the results of quantitative and semiquantitative evaluation of spectra (Kamada *et al*., 1994; Mascalchi *et al*., 2002*b*). The non-significant changes in T2 relaxation times in the cerebellum and pons of our SCA1 and SCA2 patients indicate that these changes are not a general phenomenon and that, for the purpose of metabolite quantification in these regions and in these conditions, a single TE spectrum could suffice, enabling a considerable shortening of the ^{1}H-MRS acquisition times.

Overall, we did not observe significant differences between SCA1 and SCA2 for any of the MR features. This is in line with the substantial macroscopic similarity of the neurodegenerative process in SCA1 and SCA2 (Lowe *et al*., 1997; Iwabuchi *et al*., 1999).

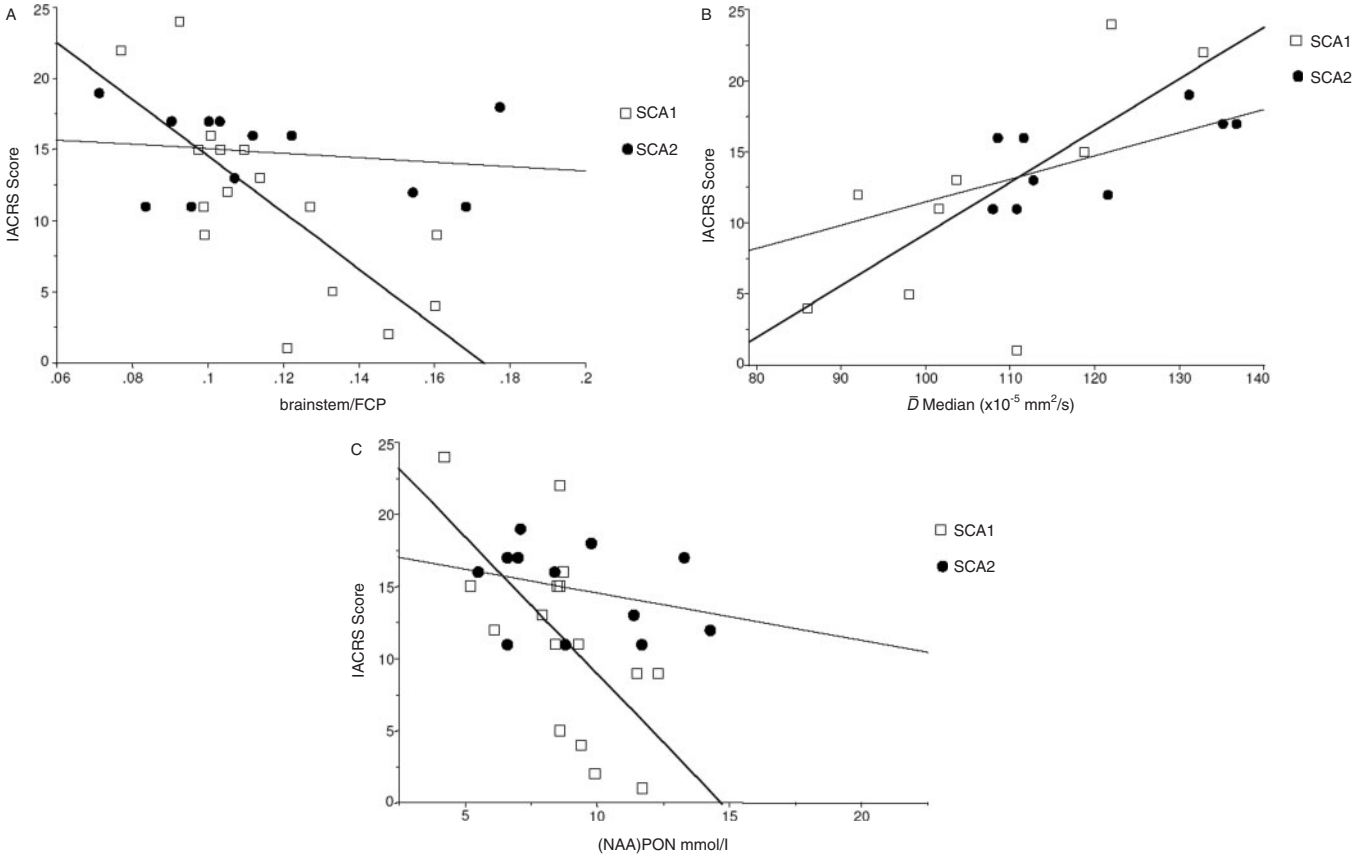

Fig. 3 Data illustrating the relationship between the IACRS score and the volumes of the brainstem normalized to the PCF (**A**), the median of the brainstem and cerebellar $\bar{D}$ (**B**) and the concentration of NAA in the pons (**C**) and in SCA1 patients (open squares) and SCA2 patients (filled circles). A significant ($P < 0.05$) correlation between clinical severity and the three MR parameters is observed for SCA1 (thick lines) ($r = -0.74$ in **A**; $r = 0.70$ in **B**; $r = -0.63$ in **C**) but not for SCA 2 (thin lines).

The second purpose of our study was to explore the relationship between MR and clinical findings in patients with SCA1 and SCA2. The severity of the neurological signs was assessed with a dedicated scale (Filla *et al*., 1990) which includes evaluation of corticospinal changes that are commonly observed in patients with SCA1 and SCA2.

In our sample we found a correlation between the severity of the neurological signs and the disease duration in SCA1 but not in SCA2. However, Filla *et al*. (1999) found a correlation between the severity of brainstem and cerebellar signs and disease duration in 30 families with SCA2.

In three previous studies, MRI-based morphometry measurements (Burk *et al*., 1996; Nagaoka *et al*., 1999) or subjective evaluations of brainstem and cerebellar atrophy (Giuffrida *et al*., 1999) were analysed with respect to disease duration, and no correlation was found in either SCA1 or SCA2. In these studies the correlation with the severity of neurological deficits was not assessed. In a recent study using a different approach with voxel-based morphometry, an inverse correlation was found between the cerebellar grey matter volume of both hemispheres and the severity of cerebellar signs in nine patients with SCA2 (Brenneis *et al*., 2003).

In a prior study we found a correlation between the median of the $\bar{D}$ in the brainstem and cerebellum in SCA1 and SCA2, considered altogether, and the IACRS score (Della Nave *et al*., 2004).

In prior ^{1}H-MRS studies of patients with SCA1 or SCA2, detailed quantitative scales of the neurological deficit were not used to address the clinical correlation.

We found a correlation between the loss of bulk, increased $\bar{D}$ and decreased NAA concentration in the brainstem on the one hand and the severity of the neurological deficit on the other hand in SCA1 but not in SCA2. In our opinion, three hypothetical explanations for this discrepancy can be proposed.

First, the different correlation between brainstem MR findings and IACRS scores in SCA1 and SCA2 could reflect the microscopic neuropathological data (Iwabuchi *et al*., 1999) showing that the damage of the brainstem grey nuclei and white matter tracts is predominant in SCA1 compared with SCA2.

Secondly, the lack of correlation in our SCA2 patients could be due to the relatively narrow range of severity of the neurological deficit (IACRS score from 12 to 19) in these patients compared with that observed in our SCA1 patients (IACRS score from 3 to 24). However, this hypothesis,

which deserves to be addressed in further studies with greater sample size, is at variance with the observation that, in our study, SCA1 patients had shorter and SCA2 patients longer disease duration. This would suggest a different temporal progression of neurodegeneration in SCA1 and SCA2, which is in line with the observation that the clinical deficit has a later onset and faster progression in SCA1 and an earlier onset and slower progression in SCA2 (Klockgether *et al*., 1998*a*). Moreover, MRI (Schols *et al*., 1997) and the pathological examination (Estrada *et al*., 1999) demonstrate earlier and more pronounced brainstem and cerebellar atrophy in SCA2 than in SCA1. These elements support the third hypothesis—that the discrepancy might reflect a different progression of neurodegeneration in SCA1 and SCA2, with an earlier onset and slower progression, consistent with a relatively indolent process, in SCA2 and later onset and faster progression, consistent with a relatively aggressive process, in SCA1. We speculate that functional compensation based on neuronal plasticity might be more efficient in limiting the clinical impact of the neurodegeneration in SCA2. Functional MRI might provide relevant insights into the pathophysiology of degenerative ataxias and is currently under evaluation in our institute.

In our series, the volume of the cerebellum and the concentration of NAA in the dentate and peridentate region were reduced in patients with SCA1 and SCA2, but no correlation with the severity of the neurological deficit was observed. However, there was a correlation between the loss of volume of the cerebellum (and also the increase in brainstem and cerebellar mean diffusivity in SCA1) and disease duration in SCA1 and SCA2. The lack of correlation between NAA concentration in the dentate and peridentate region and clinical deficit in SCA2 is not unexpected taking into account the location of our cerebellar voxel and the sparing of the dentate found on neuropathological examination in SCA2. More difficult to explain is the lack of correlation between the cerebellar volume and the clinical deficit in SCA1 and SCA2, and between the cerebellar NAA concentration and the clinical deficit in SCA1. These negative results might arise from the choice we made in terms of volumetric MRI measurements and the location of the single voxel for ^{1}H-MRS. Other MR features which were not assessed in our study, such as the volume of the vermis (Klockgether *et al*., 1998*a*) and the NAA concentration of the cerebellar cortex (Mascalchi *et al*., 2002*a*) might correlate better with the clinical deficit and deserve further investigation. Moreover quantitative proton MR spectroscopic imaging, which enables a panoramic evaluation of the brainstem and cerebellum with smaller voxel size compared with the single-voxel technique, (Jacobs *et al*., 2001) could be especially suited for this purpose.

In triplet neurodegenerative diseases as SCA1 and SCA2, the number of triplet expansions is significantly correlated with age at onset and the rate of progression of the disease (Giunti *et al*., 1998; Filla *et al*., 1999; Martin, 1999). We did not evaluate the correlation of MR findings with triplet numbers. However, in two prior studies no correlation between the number of triplets and the severity of brainstem and cerebellar atrophy was found (Klockgether 1998*b*; Giuffrida *et al*., 1999).

The correlation between degeneration of the brainstem, as detected by volumetric and diffusion MRI and quantitative ^{1}H-MRS, and the severity of neurological deficit in our SCA1 patients indicates that MR could assess disease progression in longitudinal studies of this condition. Moreover, our results support the view that MR might be employed as an outcome measure beside quantitative clinical and paraclinical tests (Velazquez Perez *et al*., 2001; Yabe *et al*., 2001; Schulte *et al*., 2002; Sakai and Miyoshi 2002) in future therapeutic trials in SCA1 driven by advances in the molecular pathology of this condition (Martin, 1999; Humbert and Saudou, 2002; Okazawa *et al*., 2002). For this purpose, diffusion MRI and ^{1}H-MRS might be more sensitive markers (Kalra *et al*., 1998) than volumetric MRI since they can give information about the condition of the surviving tissue compared with a measure (brain volume) of the irreversible tissue loss. Obviously, this requires preliminary estimation of the evolution of the volumetric, diffusion and spectroscopy changes in longitudinal studies of untreated patients, which are not available yet, and standardization of the MR techniques in the case of a multicentre trial.

In conclusion, our study indicates that both SCA1 and SCA2 are characterized by loss of bulk, increased mean diffusivity and a decrease in the concentration of NAA in the brainstem and cerebellum. The changes in the brainstem correlate with the neurological deficit in SCA1 and could be employed as measures of the severity and progression of this condition.

Acknowledgements

The MRUI software package was kindly provided by the participants in the EU Network programmes Human Capital and Mobility, CHRX-CT94-0432 and Training and Mobility of Researchers, ERB-FMRX-CT970160. This study was supported in part by a 2001 grant from the National Ataxia Foundation (Minneapolis, USA).

References

Boesch SM, Schocke M, Burk K, Hollosi P, Fornai F, Aichner FT, et al. Proton magnetic resonance spectroscopic imaging reveals differences in spinocerebellar ataxia types 2 and 6. J Magn Reson Imaging 2001; 13: 553–9.

Bozzali M, Franceschi M, Falini A, Pontesilli S, Cercignani M, Magnani G, et al. Quantification of tissue damage in AD using diffusion tensor and magnetization transfer MRI. Neurology 2001; 57: 1135–7.

Brenneis C, Bosch SM, Schocke M, Wenning GK, Poewe W. Atrophy pattern in SCA2 determined by voxel-based morphometry. Neuroreport 2003; 14: 1799–802.

Burk K, Abele M, Fetter M, Dichgans J, Skalej M, Laccone F, et al. Autosomal dominant cerebellar ataxia type I. Clinical features and MRI in families with SCA1, SCA2 and SCA3. Brain 1996; 119: 1497–505.

Cercignani M, Bozzali M, Iannucci G, Comi G, Filippi M. Magnetisation transfer ratio and mean diffusivity of normal appearing white and grey matter from patients with multiple sclerosis. J Neurol Neurosurg Psychiatry 2001; 70: 311–7.

Cercignani M, Bammer R, Sormani MP, Fazekas F, Filippi M. Inter-sequence and inter-imaging unit variability of diffusion-tensor MR imaging histogram-derived metrics of the brain in healthy volunteers. AJNR Am J Neuroradiol 2003; 24: 638–43.

Chun T, Filippi CG, Zimmerman RD, Ulug AM. Diffusion changes in the aging human brain. AJNR Am J Neuroradiol 2000; 21: 1078–83.

Davie CA, Barker GJ, Webb S, Tofts PS, Thompson AJ, Harding AE, et al. Persistent functional deficit in multiple sclerosis and autosomal dominant cerebellar ataxia is associated with axon loss. Brain 1995; 118: 1583–92.

Della Nave R, Foresti S, Tessa C, Moretti M, Ginestroni A, Gavazzi C, et al. ADC mapping of neurodegeneration in the brainstem and cerebellum of patients with progressive ataxias. Neuroimage. 2004; 22: 298–709.

Durr A, Smadja D, Cancel G, Lezin A, Stevanin G, Mikol J, et al. Autosomal dominant cerebellar ataxia type I in Martinique (French West Indies). Clinical and neuropathological analysis of 53 patients from three unrelated SCA2 families. Brain 1995; 118: 1573–81.

Estrada R, Galarraga J, Orozco G, Nodarse A, Auburger G. Spinocerebellar ataxia 2 (SCA2): morphometric analyses in 11 autopsies. Acta Neuropathol (Berl) 1999; 97: 306–10.

Filla A, De Michele G, Caruso G, Marconi R, Campanella G. Genetic data and natural history of Friedreich's disease: a study of 80 Italian patients. J Neurol 1990; 237: 345–51.

Filla A, De Michele G, Santoro L, Calabrese O, Castaldo I, Giuffrida S, et al. Spinocerebellar ataxia type 2 in southern Italy: a clinical and molecular study of 30 families. J Neurol 1999; 246: 467–71.

Gill SS, Small RK, Thomas DG, Patel P, Porteous R, Van Bruggen N, et al. Brain metabolites as 1H NMR markers of neuronal and glial disorders. NMR Biomed 1989; 2: 196–200.

Gilman S, Sima AA, Junck L, Kluin KJ, Koeppe RA, Lohman ME, et al. Spinocerebellar ataxia type1 with multiple system degeneration and glial cytoplasmic inclusions. Ann Neurol 1996; 39: 241–55.

Giuffrida S, Saponara R, Restivo DA, Trovato Salinaro A, Tomarchio L, Pugliares P, et al. Supratentorial atrophy in spinocerebellar ataxia type 2: MRI study of 20 patients. J Neurol 1999; 246: 383–8.

Giunti P, Sabbadini G, Sweeney MG, Davis MB, Veneziano L, Mantuano E, et al. The role of the SCA2 trinucleotide repeat expansion in 89 autosomal dominant cerebellar ataxia families. Frequency, clinical and genetic correlates. Brain 1998; 121: 459–67.

Gudmundsson KR. Prevalence and occurrence of some rare neurological diseases in Iceland. Acta Neurol Scand 1969; 45: 114–8.

Harding AE, Deufel T, editors. Inherited ataxias. Advances in Neurology, Vol. 61. New York: Raven Press: 1993.

Humbert S, Saudou F. Toward cell specificity in SCA1. Neuron 2002; 34: 669–70.

Iwabuchi K, Tsuchiya K, Uchihara T, Yagishita S. Autosomal dominant spinocerebellar degenerations. Clinical, pathological, and genetic correlations. Rev Neurol (Paris) 1999; 155: 255–70.

Jacobs MA, Horska A, Van Zijl PCM, Barker PB. Quantitative proton MR spectroscopic imaging of normal human cerebellum and brainstem. Magn Reson Med 2001; 46: 699–705.

Kalra S, Cashman NR, Genge A, Arnold DL. Recovery of N-acetylaspartate in corticomotor neurons of patients with ALS after riluzole therapy. Neuroreport 1998; 9: 1757–61.

Kamada K, Houkin K, Hida K, Matsuzawa H, Iwasaki Y, Abe H, Nakada T. Localized proton spectroscopy of focal brain pathology in humans: significant effects of edema in spin-spin relaxation time. Magn Reson Med 1994; 31: 537–40.

Klockgether T, Ludtke R, Kramer B, Abele M, Burk K, Schols L, et al. The natural history of degenerative ataxia: a retrospective study in 466 patients. Brain 1998a; 121: 589–600.

Klockgether T, Skalej M, Wedekind D, Luft AR, Welte D, Schulz JB, et al. Autosomal dominant cerebellar ataxia type I. MRI-based volumetry of posterior fossa structures and basal ganglia in spinocerebellar ataxia types 1, 2 and 3. Brain 1998b; 121: 1678–93.

Lowe J, Lennox G, Leigh PN. Disorders of movement and system degeneration. In: Graham DL, Lantos PL, editors. Greenfield's neuropathology, Vol. 2 . 6th ed. London: Arnold; 1997. p. 281–366.

Martin JB. Molecular basis of the neurodegenerative disorders. N Engl J Med 1999; 340: 1970–80.

Mascalchi M, Tosetti M, Plasmati R, Bianchi MC, Tessa C, Salvi F, et al. Proton magnetic resonance spectroscopy in an Italian family with spinocerebellar ataxia type 1. Ann Neurol 1998; 43: 244–52.

Mascalchi M, Brugnoli R, Guerrini L, Belli G, Nistri M, Politi LS, et al. Single voxel long TE 1H-MR spectroscopy of the normal brainstem and cerebellum. J Magn Reson Imaging 2002a; 16: 532–7.

Mascalchi M, Belli G, Guerrini L, Nistri M, Del Seppia I, Villari N. Proton MR spectroscopy of Wernicke's encephalopathy. AJNR Am J Neuroradiol 2002b; 23: 1803–6.

Nagaoka U, Suzuki Y, Kawanami T, Kurita K, Shikama Y, Honda K, et al. Regional differences in genetic subgroup frequency in hereditary cerebellar ataxia, and a morphometrical study of brain MR images in SCA1, MJD and SCA6. J Neurol Sci 1999; 164: 187–94.

Okazawa H, Rich T, Chang A, Lin X, Waragai M, Kajikawa M, et al. Interaction between mutant ataxin-1 and PQBP-1 affects transcription and cell death. Neuron 2002; 34: 701–13.

Ormerod IEC, Harding AE, Miller DH, Johnson G, Mac Manus D, du Boulay EP, et al. Magnetic resonance imaging in degenerative ataxic disorders. J Neurol Neurosurg Psychiatry 1994; 57: 51–7.

Pareyson D, Gellera C, Castellotti B, Antonelli A, Riggio MC, Mazzucchelli F, et al. Clinical and molecular studies in 73 Italian families with autosomal dominant cerebellar ataxia type I: SCA1 and SCA2 are the most common genotypes. J Neurol 1999; 246: 389–93.

Raz N, Gunning-Dixon F, Head D, Williamson A, Acker JD. Age and sex differences in the cerebellum and the ventral pons: a prospective MR study of healthy adults. AJNR Am J Neuroradiol 2001; 22: 1161–7.

Sakai T, Miyoshi K. The use of quantitative methods in clinical trials for spinocerebellar ataxia [letter]. Arch Neurol 2002; 59: 1044–5.

Savoiardo M, Strada L, Girotti F, Zimmerman RA, Grisoli M, Testa D, et al. Olivopontocerebellar atrophy: MR diagnosis and relationship to multisystem atrophy. Radiology 1990; 174: 693–6.

Schols L, Amoiridis G, Buttner T, Przuntek H, Epplen JT, Riess O. Autosomal dominant cerebellar ataxia: phenotypic differences in genetically defined subtypes? Ann Neurol 1997; 42: 924–32.

Schulte T, Mattern R, Berger K, Szymanski S, Klotz P, Kraus PH, et al. Double-blind crossover trial of trimethoprim-sulfamethoxazole in spinocerebellar ataxia type3/Machado–Joseph disease. Arch Neurol 2001; 58: 1451–7.

Subramony SH, Filla A. Autosomal dominant spinocerebellar ataxia ad infinitum? Neurology 2001; 56: 287–9.

Ulug AM, Grunewald T, Lin MT, Kamal AK, Filippi CG, Zimmerman RD, et al. Diffusion tensor imaging in the diagnosis of primary lateral sclerosis. J Magn Reson Imaging 2004; 19: 34–9.

van de Warrenburg BPC, Sinke RJ, Verschuuren-Bemelmans CC, Scheffer H, Brunt ER, Ippel PF, et al. Spinocerebellar ataxias in the Netherlands. Prevalence and age at onset variance analysis. Neurology 2002; 58: 702–8.

van den Boogaart A, van Ormondt D, Pijnappel WWF, de Beer R, Ala-Korpela M. In: McWhirter JG, editor. Mathematics in signal processing III. Oxford: Clarendon Press; 1994. p. 175–95.

van den Boogaart A, Van Hecke A, Van Huffel S, Graveron-Demilly S, van Ormondt D, de Beer R. MRUI: a graphical user interface for accurate routine MRS data analysis [abstract]. In: Proceedings of the European Society of Magnetic Resonance in Medicine and Biology 13th Annual Meeting, Prague. 1996. p. 318.

Vanhamme L, van den Boogaart A, Van Huffel S. Improved method for accurate and efficient quantification of MRS data with use of prior knowledge. J Magn Reson 1997; 129: 35–43.

Velazquez Perez L, De La Hoz Oliveras J, Perez Gonzalez R, Hechevarria Pupo RR, Herrera Dominguez H. Quantitative evaluation of disorders of coordination in patients with Cuban type 2 spinocerebellar ataxia. Rev Neurol 2001; 32: 601–6.

Wullner U, Klockgether T, Petersen D, Naegele T, Dichgans J. Magnetic resonance imaging in hereditary and idiopathic ataxia. Neurology 1993; 43: 318–26.

Yabe I, Sasaki H, Yamashita I, Takei A, Tashiro K. Clinical trial of acetazolamide in SCA6, with assessment using the Ataxia Rating Scale and body stabilometry. Acta Neurol Scand 2001; 104: 44–7.